9788 *Inorg. Chem.* **2010**, *49*, 9788–9797
DOI: 10.1021/ic100581k

Inorganic Chemistry
Article

Synthesis, Crystal Structure, Quantum Chemical Calculations, DNA Interactions, and Antimicrobial Activity of [Ag(2-amino-3-methylpyridine)$_2$]NO_3 and [Ag(pyridine-2-carboxaldoxime)NO_3]

Morsy A. M. Abu-Youssef,*,† Saied M. Soliman,† Vratislav Langer,‡ Yousry M. Gohar,§ Ahmed A. Hasanen,† Mohamed A. Makhyoun,† Amira H. Zaky,∥ and Lars R. Öhrström*,‡

†*Department of Chemistry, Faculty of Science, Alexandria University, P.O. Box 426 Ibrahimia, 21321 Alexandria, Egypt,* ‡*Department of Chemical and Biological Engineering, Chalmers University of Technology, SE-41296 Gothenburg, Sweden,* §*Deptartment of Microbiology, Faculty of Science, Alexandria University, Alexandria, Egypt, and* ∥*Deptartment of Biochemistry, Faculty of Science, Alexandria University, Alexandria, Egypt*

Received March 28, 2010

[Ag(2-amino-3-methylpyridine)$_2$]NO_3 (**1**) and [Ag(pyridine-2-carboxaldoxime)NO_3] (**2**) were prepared from corresponding ligands and $AgNO_3$ in water/ethanol solutions, and the products were characterized by IR, elemental analysis, NMR, and TGA. The X-ray crystal structures of the two compounds show that the geometry around the silver(I) ion is bent for complex **1** with nitrate as an anion and trigonal planar for complex **2** with nitrate coordinated. ESI-MS results of solutions of **2** indicate the independent existence in solution of the [Ag(pyridine-2-carboxaldoxime)]$^+$ ion. The geometries of the complexes are well described by DFT calculations using the ZORA relativistic approach. The compounds were tested against 14 different clinically isolated and four ATCC standard bacteria and yeasts and also compared with 17 commonly used antibiotics. Both **1** and **2** exhibited considerable activity against *S. lutea*, *M. lutea*, and *S. aureus* and against the yeast *Candida albicans*, while 2-amino-3-methylpyridine is slightly active and pyridine-2-carboxaldoxime shows no antimicrobial activity. In addition, the interaction of these metal complexes with DNA was investigated. Both **1** and **2** bind to DNA and reduce its electrophoretic mobility with different patterns of migration, while the ligands themselves induce no change.

Silver(I) coordination chemistry has attracted attention in recent decades for mainly two reasons: (1) Ag(I) adopts various coordination numbers and geometries (i.e., linear, trigonal−planar, or tetrahedral) and also forms argentophilic interactions; synthesis of Ag(I) coordination network solids has produced many novel and unexpected network topologies.[1,2] (2) Prompted by the increase in multidrug resistant bacteria,[3] the use of new wound dressing materials using the antimicrobial properties of Ag^+ ions has been a strong trend.[4,5]

The latter motivation is by no means new. Silver was used as an antimicrobial agent for a long time before the discovery of microorganisms,[6] and in "modern" medicine, prior to the introduction of efficient antibiotics, silver in various forms was used in a number of clinical situations. However, since World War II, its use has declined; for example, the compulsory dropping of $AgNO_3$ solutions in the eyes of newly born babies was discontinued in Sweden during the 1980s.[7] Although some of these practices were not documented and verified according to modern standards, the antimicrobial activity of the silver(I) ion is nevertheless real,[8] and the topical use of silver nitrate for the prevention of infections in burns and hard-to-heal wounds was revived in the 1960s, although its clinical effects were not undisputed.[9]

The introduction of the nowadays commonly used drug silver sulfadiazine ([Ag((4-aminophenyl)sulfonyl)(pyrimidin-2-yl)azanide]$_n$, also know under different trade names) in 1968 appeared to be an improvement,[9] and more recently, wound healing concepts based on other silver preparations, including

*To whom correspondence should be addressed. Tel:+203 5917883 (M.A.M.A.-Y.), +31 772 1000 (L.R.Ö.). Fax: +203 5932488 (M.A.M.A.-Y.), +46 31 772 3858 (L.R.Ö.). E-mail: morsy5@link.net (M.A.M.A.-Y.), ohrstrom@chalmers.se (L.R.Ö.).

(1) Khlobystov, A. N.; Blake, A. J.; Champness, N. R.; Lemenovskii, D. A.; Majouga, A. G.; Zyk, N. V.; Schroder, M. *Coord. Chem. Rev.* **2001**, *222*, 155.
(2) Abu-Youssef, M. A. M.; Langer, V.; Öhrström, L. *Chem. Commun.* **2006**, 1082.
(3) *The bacterial challenge: time to react European Centre for Disease Prevention and Control*; ECDC/EMEA Joint Technical Report, EMEA doc. ref. EMEA/576176/2009: London, **2009**; ISBN: 978-92-9193-193-4, DOI: 10.2900/2518.
(4) Chopra, I. *J. Antimicrob. Chemother.* **2007**, *59*, 587.
(5) Edwards-Jones, V. *Lett. Appl. Microbiol.* **2009**, *49*, 147.
(6) Klasen, H. J. *Burns* **2000**, *26*, 117.
(7) Stams, D. A.; Thomas, T. D.; MacLaren, D. C.; Ji, D.; Morton, T. H. *J. Am. Chem. Soc.* **1990**, *112*, 1427.
(8) Silver, S.; Phung, L. T.; Silver, G. *J Ind. Microbiol. Biotechnol.* **2006**, *33*, 627.
(9) Klasen, H. J. *Burns* **2000**, *26*, 131.

 Published on Web 10/07/2010

"nanosilver",[3,4] have been introduced. A common problem for all of these dressings is, however, the lack of proven clinical efficiency in randomized controlled trials.[8,10,11] Consequently, much work is still needed, both in the laboratory and the clinic, until we have the ultimate way of harvesting the antimicrobial properties of silver compounds.

One should also notice that the promotion of "colloidal silver", and other silver preparations advocated by "alternative" medicine, seems to have no scientific basis, and claims that silver has a positive stimulating or synergistic action effect on the human immune system are, as far as we know, groundless. Moreover, silver has no known definite role in any biological system. On the contrary, continuous exposure to silver as a "nutritional supplement" might have adverse effects despite the known low toxicity of the silver(I) ion. In addition, bacteria do develop resistance to silver,[10,12] and therefore the use of silver in everyday devices where it is merely convenient to stop bacterial growth but where normal hygienic practices are actually sufficient, such as in socks and refrigerators, should not be encouraged. Thus, the biological activity of new silver(I) complexes is potentially important, and these compounds are developed not only with wound care in mind[13−31] but also with the treatment of lungs chronically infected with cystic fibrosis.[32,33]

Scheme 1. Ligands Used in This Study: 2-Amino-3-methylpyridine (2am3Mepy) and Pyridine-2-carboxaldoxime (py2ald)

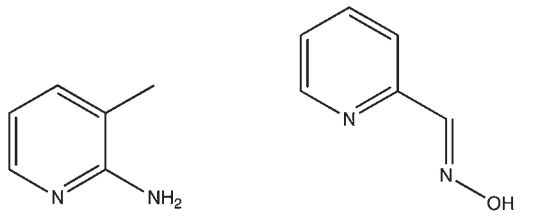

2-amino-3-methylpyridine (*E*)-pyridine-2-carboxaldoxime

Our group has previously reported silver compounds with nicotinic acid derivatives active against clinical isolates of multidrug resistant (MDR) bacterial strains of four pathogenic bacteria: *Staphylococcus aureus*, *Streptococcus pyogenes*, *Proteus mirabilis*, and *Pseudomonas aeruginosa*,[34] and in all cases except for *S. aureus*, where the activity was similar, these compounds outperformed, *in vitro*, the still widely used silver sulfadiazine.[9] Here, we present the synthesis, X-ray structure, DFT optimized geometry, experimental and calculated vibrational spectra, thermal behavior, interaction with DNA, and antimicrobial properties of [Ag(2-amino-3-methylpyridine)$_2$]-NO_3 (**1**) and Ag(pyridine-2-carboxaldoxime) NO_3] (**2**; see Scheme 1) against 14 different clinically isolated MDR bacteria and four ATCC standard bacteria and a yeast.

Experimental Section

Synthesis. All chemicals were reagent grade and used without further purification.

[Ag(2-amino-3-methylpyridine)$_2$]NO_3, 1. To a stirred solution of $AgNO_3$ (0.170 g, 1.0 mmol) in 10 mL of deionized water was added dropwise an ethanolic solution of 2-amino-3-methylpyridine (0.108 g, 1.0 mmol) over 20 min. The clear solution was subsequently placed in a refrigerator at ∼4 °C for a several days to give colorless, plated crystals suitable for X-ray measurements. The crystals were filtered off, washed with a small amount of ethanol, and dried in the air. Yield: 0.293 g, 76% with respect to the ligand. Analytical data (%), Calcd: C, 37.29; H, 4.14; N, 18.13; Ag, 27.93. Found: C, 37.33; H, 4.33; N, 18.06; Ag, 28.16. ^{1}H NMR (DMSO-*d*6): 2.06 (s, 3H, CH_3 at *m*-position of Py), 6.27 (s, 2H, NH_2 at *o*-position of Py), 6.54 (t, 1H, *m*-H of Py), 7.37 (d, 1H, *p*-H of Py), 7.87 (d, 1H, *o*-H of Py). ^{13}C NMR (DMSO-*d*6): 17.91 (CH_3 at C3), 113.10 (C5 of Py), 118.58 (C3 of Py), 138.90 (C6 of Py), 146.99 (C4 of Py), 158.57 (C2 of Py).

[Ag(pyridine-2-carboxaldoxime)NO_3], 2. $AgNO_3$ (0.170 g, 1.00 mmol) dissolved in 10 mL of water was mixed with 15 mL of ethanol containing pyridine-2-carboxaldoxime (0.122 g, 1.00 mmol). The solution was well shaken for one minute and then kept at ambient temperature and protected from the light. After two weeks, colorless long needles were obtained. The crystals were filtered off and washed with a water/ethanol solution (1:10) and subsequently air-dried to give 0.24 g of **2** (82% with respect to the ligand). Analytical data (%), Calcd.: C, 24.66; H, 2.05; N, 14.38; Ag, 36.94. Found: C, 24.82; H, 2.35; N, 14.43; Ag, 37.02. ^{1}H NMR (DMSO-*d*6): 7.54 (t, 1H, *m*-position of Py), 7.75(d, 1H, *o*-position of Py), 7.99 (t, 1H, *p*-H of Py), 8.60(d, 1H, *m*-H of Py), 8.35 (s, 1H, of oxime carbon), 12.14 (s, 1H, of hydroxide). ^{13}C NMR (DMSO-*d*6): 124.68 (C_3 of Py), 126.30 (C_5), 139.35 (C_4 of Py), 148.35 (oxime carbon), 150.20(C_6 of Py), 151.30 (C_2 of Py). ESI-MS: *m*/*z* 228.9585. Calcd: 228.9526 for $C_6H_6N_2AgO$

(10) Silver, S. *FEMS Microbiol. Rev.* **2003**, *27*, 341.
(11) Storm-Versloot, M. N.; Vos, C. G.; Ubbink, D. T.; Vermeulen, H. *Topical silver for preventing wound infection*; The Cochrane Collaboration, John Wiley & Sons. Ltd: New York, 2010.
(12) Brett, D. W. *Ostomy Wound Manage.* **2006**, *52*, 34.
(13) McCann, M.; Coyle, B.; Briody, J.; Bass, F.; O'Gorman, N.; Devereux, M.; Kavanagh, K.; McKee, V. *Polyhedron* **2003**, *22*, 1595.
(14) Chen, S. P.; Wu, G. Z.; Zeng, H. Y. *Carbohydr. Polym.* **2005**, *60*, 33.
(15) Nomiya, K.; Yoshizawa, A.; Tsukagoshi, K.; Kasuga, N. C.; Hirakawa, S.; Watanabe, J. *J. Inorg. Biochem.* **2004**, *98*, 46.
(16) Kasuga, N. C.; Sugie, A.; Nomiya, K. *Dalton Trans.* **2004**, 3732.
(17) Djokic, S. S. *J. Electrochem. Soc.* **2004**, *151*, C359.
(18) Devereux, M.; McCann, M.; Shea, D. O.; Kelly, R.; Egan, D.; Deegan, C.; Kavanagh, K.; McKee, V.; Finn, G. *J. Inorg. Biochem.* **2004**, *98*, 1023.
(19) Coyle, B.; McCann, M.; Kavanagh, K.; Devereux, M.; McKee, V.; Kayal, N.; Egan, D.; Deegan, C.; Finn, G. J. *J. Inorg. Biochem.* **2004**, *98*, 1361.
(20) Abuskhuna, S.; Briody, J.; McCann, M.; Devereux, M.; Kavanagh, K.; Fontecha, J. B.; McKee, V. *Polyhedron* **2004**, *23*, 1249.
(21) Tsyba, I.; Mui, B. B. K.; Bau, R.; Noguchi, R.; Nomiya, K. *Inorg. Chem.* **2003**, *42*, 8028.
(22) Tavman, A.; Ulkuseven, B.; Birteksoz, S.; Otuk, G. *Folia Microbiol.* **2003**, *48*, 479.
(23) Balogh, L.; Swanson, D. R.; Tomalia, D. A.; Hagnauer, G. L.; McManus, A. T. *Nano Lett.* **2001**, *1*, 18.
(24) Ulkuseven, B.; Tavman, A.; Otuk, G.; Birteksoz, S. *Folia Microbiol.* **2002**, *47*, 481.
(25) Creaven, B. S.; Egan, D. A.; Kavanagh, K.; McCann, M.; Mahon, M.; Noble, A.; Thati, B.; Walsh, M. *Polyhedron* **2005**, *24*, 949.
(26) Melaiye, A.; Sun, Z. H.; Hindi, K.; Milsted, A.; Ely, D.; Reneker, D. H.; Tessier, C. A.; Youngs, W. J. *J. Am. Chem. Soc.* **2005**, *127*, 2285.
(27) Dias, H. V. R.; Batdorf, K. H.; Fianchini, M.; Diyabalanage, H. V. K.; Carnahan, S.; Mulcahy, R.; Rabiee, A.; Nelson, K.; van Waasbergen, L. G. *J. Inorg. Biochem.* **2006**, *100*, 158.
(28) Noguchi, R.; Hara, A.; Sugie, A.; Nomiya, K. *Inorg. Chem. Commun.* **2006**, *9*, 60.
(29) Barreiro, E.; Casas, J. S.; Couce, M. D.; Sanchez, A.; Seoane, R.; Sordo, J.; Varela, J. M.; Vazquez-Lopez, E. M. *Eur. J. Med. Chem.* **2008**, *43*, 2489.
(30) Galal, S. A.; Hegab, K. H.; Kassab, A. S.; Rodriguez, M. L.; Kerwin, S. M.; El-Khamry, A. M. A.; El Diwani, H. I. *Eur. J. Med. Chem.* **2009**, *44*, 1500.
(31) Panzner, M. J.; Hindi, K. M.; Wright, B. D.; Taylor, J. B.; Han, D. S.; Youngs, W. J.; Cannon, C. L. *Dalton Trans.* **2009**, 7308.
(32) Hindi, K. M.; Siciliano, T. J.; Durmus, S.; Panzner, M. J.; Medvetz, D. A.; Reddy, D. V.; Hogue, L. A.; Hovis, C. E.; Hilliard, J. K.; Mallet, R. J.; Tessier, C. A.; Cannon, C. L.; Youngs, W. J. *J. Med. Chem.* **2008**, *51*, 1577.
(33) Hindi, K. M.; Ditto, A. J.; Panzner, M. J.; Medvetz, D. A.; Han, D. S.; Hovis, C. E.; Hilliard, J. K.; Taylor, J. B.; Yun, Y. H.; Cannon, C. L.; Youngs, W. J. *Biomaterials* **2009**, *30*, 3771.
(34) Abu-Youssef, M. A. M.; Dey, R.; Massoud, A. A.; Gohar, Y.; Langer, V.; Öhrström, L. *Inorg. Chem.* **2007**, *46*, 5893.

Table 1. Crystallographic Data and Refinement Parameters

	1	2
empirical formula	$AgC_{12}H_{16}N_4.NO_3$	$AgC_6H_6N_2O_1.NO_3$
fw	386.17	292.01
temp	173(2) K	173(2) K
wavelength	0.71073 Å	0.71073 Å
cryst syst	triclinic	orthorhombic
space group	$P\bar{1}$ (No.2)	$P2_12_12_1$
unit cell dimensions (Å, deg)	a = 8.0051 (1)	a = 3.6340(2)
	b = 9.6087 (1)	b = 14.5915(8)
	c = 10.2115 (2)	c = 16.0754(9)
	α = 91.609 (1)	α = 90
	β = 96.946 (1)	β = 90
	γ = 109.105 (1)	γ = 90
V (Å^3)	734.825 (19)	852.41(8)
Z	2	4
density, calc. (Mg/m^3)	1.745	2.275
absorption coeff (mm^{-1})	1.389	2.356
F(000)	388	568
cryst size (mm^3)	0.28 × 0.14 × 0.07	0.88 × 0.18 × 0.16
θ range (deg)	2.25 to 25.05	2.53 to 33.03
reflns collected	7874	12438
independent reflns	2613 [R(int) = 0.0559]	3067 [R(int) = 0.0201]
completeness (%)/θ_{max} (deg)	99.9/25.05	99.5/30.5
absorption correction	multiscan	multiscan
max. and min. transmission	0.9090 and 0.6971	0.7043 and 0.2309
refinement method	full-matrix least-squares on F^2	full-matrix least-squares on F^2
data/restraints/params	2613/4/205	3067/0/128
goodness-of-fit on F^2	1.008	1.007
final R indices [I > 2σ(I)]	R1 = 0.0704, wR2 = 0.1800	R1 = 0.0259, wR2 = 0.0748
R indices (all data)	R1 = 0.0810, wR2 = 0.1927	R1 0.0271, wR2 = 0.0754
largest diff. peak and hole (e Å^{-3})	2.150 and −2.402	1.034 and −0.596

Materials and Instrumentation. The infrared spectra were recorded on a Bruker IFS-125 model FT-IR spectrophotometer as KBr pellets in the range of 200−4000 cm^{-1}. NMR spectra were recorded at the Central Lab., Faculty of Science, Alexandria University using a JEOL GNM ECA 500 MHz NMR spectrometer. Elemental analysis (CHN) was performed at the Microanalytical Center at Cairo University and ICP Ag analysis at the New Materials Institute "Mubarak City for Scientific Research and Technological Applications" with a Prodigy High Dispersion ICP-OES (Teledyne Leeman Laboratories, USA). Complementary silver analysis for **2** was performed with the Volhard method. For the thermal analysis, a Shimadzu thermogravimetric analyzer TGA-50H was used, measuring from ambient temperature up to 800 °C.

Electrospray Ionization Mass Spectrometry (ESI-MS). High-resolution ESI-MS analyses were performed on a Bruker APEX-Qe hybrid quadrupole Fourier transform ion cyclotron resonance (Q−FT-ICR) mass spectrometer, equipped with an Apollo-II ESI source and a 4.7-T superconducting magnet. The instrument was operated in both positive and negative ion modes. About 1 mg of **2** was dissolved in 1 mL of DMSO (2 mM), since it is sparingly soluble in water; then 0.1 mL of this solution was diluted with 4 mL of EtOH (giving a resulting solution of 0.05 mM Ag^+_{tot}). This solution was infused into the ESI source at a flow rate of 1.5 μL/min, and positive ions were detected. The instrument was operated with Bruker XMASS 7.0.8 software, and spectra were processed/analyzed with the use of Bruker DataAnalysis 3.5 software.

X-Ray Crystallography. Crystallographic measurements were made on a Siemens Smart CCD diffractometer with graphite monochromated Mo Kα radiation at 173 K. CCD data were integrated with the *SAINT* package,[35] and a multi-scan absorption correction was applied using *SADABS*.[36] All structures were solved by direct methods and refined against all F^2 data by full-matrix least-squares (*SHELXL97*[37]), including anisotropic displacement parameters for all non-H atoms. Hydrogen atoms were refined isotropically using geometrical constraints with the exception of the amino groups in **1**, where soft geometrical restraints were used. The crystallographic data are summarized in Table 1.

Testing of Antimicrobial Activity. The antimicrobial activities of **1** and **2** were determined according to the recommendations of NCCLS40[38] by the use of the broth microdilution method. Minimum inhibitory concentrations (MICs) for the tested compounds were conducted using 10 clinical isolates from diabetic foot ulcers (Department of Vascular Surgery, Faculty of Medicine, Alexandria University, Alexandria, Egypt); *Micrococcus luteus*, *Staphylococcus aureus*, and *Streptococcus pyogenes* as Gram-positive bacteria; *Escherichia coli*, *Klebsiella pneumoniae*, *Pseudomonas aeruginosa*, *Proteus mirabilis*, *Enterobacter cloacae*, and *Serratia enterica* as Gram negative bacteria, and the yeast *Cadida albicans*. Compounds **1** and **2** were also tested against the following standard bacteria from the American Type Culture Collection (ATCC): *Sarcina lutea*, ATCC 10031, *S. aureus*, ATCC 6538p, *E. coli*, ATCC 8739, and *P. aeruginosa*, ATCC 9027. The tested compounds were dissolved in DMSO to give a stock solution that was subsequently diluted in the growth medium to give 1.5 serial dilutions from 256 − 0.5 μg/mL medium. To ensure full solubility of the tested materials, 5% DMSO was present in all bioassay media, a concentration which had no antibacterial effect on its own. Bacteria were cultured in Mueller Hinton Broth (MHB) for 24 h at 35 °C with 10^5 CFU/mL culture filtrate. MIC values correspond to the lowest concentration that inhibited the bacterial growth.

Electrophoretic DNA Migration. Plasmid pGL2-basic vector DNA; electrophoresis grade boric acid; agarose; and molecular biology grade tris(hydroxymethyl)aminomethane (Tris), glycerol, and ethidium bromide were all purchased from Sigma−Aldrich.

DNA aliquots of double digested pGL2 plasmid DNA (to yield three bands of 4000, 2000, and 1000 bp, respectively) were prepared. A total of 1 μg of DNA was mixed with 2 μg of 2am3Mepy, py2ald,

(35) *SAINT*; Siemens analytical X-ray Instruments Inc.: Madison, WI, 1995.
(36) Sheldrick, G. M. *SADABS*; University of Göttingen: Göttingen, Germany, 1996.
(37) SHELXL: Sheldrick, G. M. *Acta Crystallogr.* **2008**, *A64*, 112−122.
(38) *Performance standards for antimicrobial susceptibility testing. NCCLS approved standard M100-S9*; National Committee for Clinical Laboratory Standards (NCCLS): Wayne, PA, 1999.

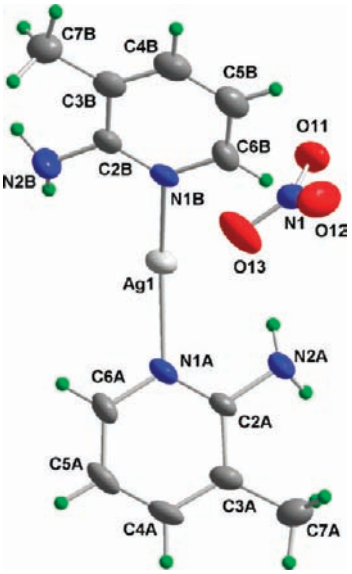

Figure 1. A displacement ellipsoids drawing (50%) of **1**, showing the atom-numbering scheme. The N1A−Ag−N1B angle is 153.2(2)°, and the shortest Ag···O distance is 2.828(2) Å.

silver nitrate, **1**, or **2**. The mixtures were completed to 7 μL by a 10 mM Tris-HCl buffer (pH 6.8) and incubated at 25 °C overnight. The 7 μL mixture was subsequently subjected to 1.5% agarose gel containing 1 μg/mL ethidium bromide for 90 min at 50 V/10 cm^2 agarose plate in 89 mM Tris−boric acid and 2 mM EDTA buffer (pH 8.0) and visualized over a UVP transilluminator.

Quantum Chemical Calculations. The geometry optimization and calculation of vibrational spectra were carried out with the density functional theory approach using the Orca software.[39,40] The optimized geometry and vibrational spectra of complexes **1** and **2** were calculated using the ZORA[41] approximation. In ZORA, a scalar relativistic approach, the ZORA approximation of the nuclear attraction term, Coulomb potential, Slater exchange potential (X-α potential with α = 0.7), and local correlation potential (VWN5 model potential) are used. The following basis sets were used.[42] C, N, O: TZV(ZORA) (11S6P/6S3P). H: TZV(ZORA) (5S/3S). Ag: TZVP (ZORA) (19S15P9d/8S7P5d).

Result and Discussion

Structure Descriptions. The crystal data and structure refinement parameters for [Ag(2-amino-3-methylpyridine)$_2$]NO_3 (**1**) and [Ag(pyridine-2-carboxaldoxime)NO_3] (**2**) are found in Table 1, and the atom numbering schemes are shown in Figures 1 and 2, respectively.

In complex **1**, silver(I) is coordinated to two pyridine moieties via the ring nitrogen atom, while the amine groups are not coordinated but are taking part in a hydrogen-bonding pattern. This leads to a slightly bent structure with a N−Ag−N bond angle of 153.2(2)°. The distance between the silver and the oxygen of the nitrate group is 2.828(2) Å, and thus the nitrate is only weakly coordinated to silver.[43] For complex **2**, the pyridine-2-carboxaldoxime acts as a bidentate ligand via the ring nitrogen and the oxime group

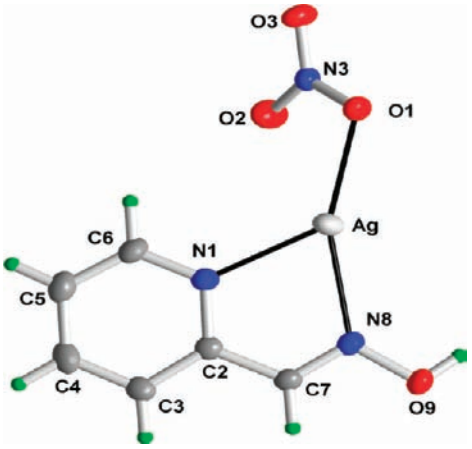

Figure 2. Numbering scheme and atomic displacement ellipsoids drawn at the 50% probability level for complex **2**. The Ag−O1 distance is 2.329(2) Å.

nitrogen atom, forming a distorted trigonal planar geometry around the silver(I) ion. The N1−Ag−N8 bond angle is 71.65(7)°, and the shorter Ag−O bond distance 2.329(2) Å indicates a stronger interaction with the coordinated nitrate group.[43] We note that only 13 structures containing AgN_2O with a N−Ag−N chelating unit can be found in the Cambridge Crystallographic Database.[44]

Table 2 compares the hydrogen bonding in compounds **1** and **2**. As stated above, in **1**, neither the nitrate nor the amine group is coordinated to silver; instead NO_3^- is hydrogen bonded to the NH_2 groups with R4,4(12) and R4,4(24) motifs forming stacks in the *a* direction, see Figure 3. These stacks are then packed with apparent $\pi-\pi$ interactions with interplanar distances of 3.293 Å and 3.493 Å.

We may speculatively interpret this behavior considering the coordinating and hydrogen bonding properties of the nitrate and amine groups. First, we note that a large part of the ligand is hydrophobic and thus needs to be separated from the more hydrophilic structure components. This can be achieved by coordinating both the nitrate and the amine to the silver ion, thus assembling all of the hydrophilic parts around silver. The alternative is that both of these groups are "free" and instead hydrogen-bond to each other, thus "protecting" them from the hydrophobic methyl groups and aromatic rings. It seems in **1** that the latter option has prevailed.

For compound **2**, a strong hydrogen bond between the hydroxyl group and the nitrate (O9−H9···O3) leads to the formation of a helical one-dimensional motif in the *a* direction, as shown in Figure 4. In this case, the $\pi-\pi$ interactions indicated by the parallel pyridine π systems with a centroid−centroid distance of 3.634 Å and tilt angles of 17.9−22.5° reinforce the chain motif, and weaker forces, i.e., C−H...O hydrogen bonds, act between the chains.

Hirshfeld Surface Analysis. This classic analysis of the crystal structures is somewhat biased by the scientists' preconceptions of what interactions may be important, as it is very time-consuming to consider all atom−atom interactions by visual inspection and measuring. In particular, weaker interactions are difficult to interpret. Spackman and co-workers have therefore developed a procedure based on

(39) Neese, F. *ORCA*, v. 2.6−63, April 2008; Lehrstuhl für Theoretische Chemie, Universität Bonn: Bonn, Germany. http://www.thch.uni-bonn.de/tc/orca/ (accessed Sep 2010).
(40) Zein, S.; Duboc, C.; Lubitz, W.; Neese, F. *Inorg. Chem.* **2008**, *47*, 134.
(41) van Wuellen, C. *J. Chem. Phys.* **1998**, *09*, 392.
(42) Schaefer, A.; Horn, H.; Ahlrichs, R. *J. Chem. Phys.* **1992**, *97*, 2571.
(43) Abu-Youssef, M. A. M.; Langer, V.; Öhrström, L. *Dalton Trans.* **2006**, 2542.
(44) Allen, F. H. *Acta Crystallogr., Sect. B* **2002**, *58*, 380.

Table 2. The Hydrogen Bond Interactions for Compounds **1** and **2**[a]

1			**2**		
bond	$r_{N\cdots O}$ (Å)	angle$_{N-H\cdots O}$ (deg)	bond	$r_{D\cdots O}$ (Å)	angle$_{O-H\cdots O}$ (deg)
N2A−H1A···O12	3.316(9)	141(7)	O9−H9···O3^{i}	2.721(3)	175
N2A−H1A···O13	3.140(9)	167(8)	C7−H7···O2^{ii}	3.353(3)	154
N2A−H2A···O11^{i}	3.036(8)	139(8)			
N2B−H1B···O12^{ii}	3.097(9)	145(8)			
N2B−H2B···O11^{iii}	3.179(9)	165(8)			

[a] Symmetry codes, **1**: (i): $-x+2, -y, -z+1$. (ii): $x-1, y, z$. (iii): $-x+1, -y, -z+1$. **2**: (i) $0.5+x, 1.5-y, 1-z$. (ii) $2-x, -0.5+y, 0.5-z$.

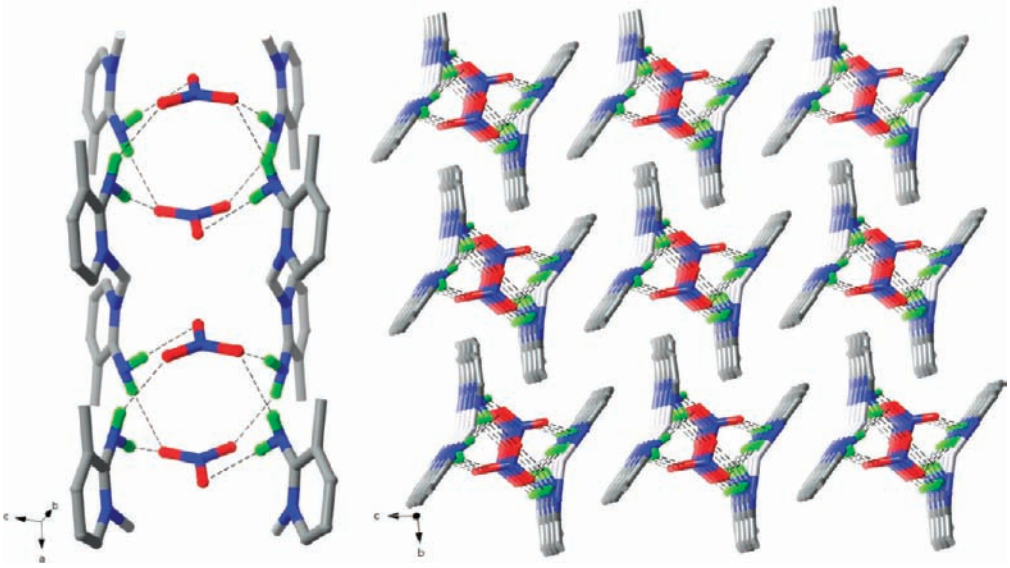

Figure 3. Left: The hydrogen-pattern (dashed lines) in **1**. All hydrophilic groups are hidden within the cores of columns running in the *a* direction. Right: These columns are then packed with $\pi-\pi$ interactions with interplanar distances of 3.293 Å and 3.493 Å. Hydrogen atoms not participating in hydrogen bonds have been omitted. See also Table 2.

Hirshfeld surfaces,[45−47] implemented in the CrystalExplorer program,[48] basically visualizing all interactions in a single picture. We have used this approach to investigate the $\pi-\pi$ interactions in **1** and **2**, and this feature is most clearly visible as a flat region on the *curvedness surface*[45] (curvedness is a function of the rms curvature of the surface), see Figures 5 and 6.

Although $\pi-\pi$ interactions were identified for both **1** and **2**, the plots in Figures 5 and 6 show some pronounced differences. We can see that in **1**, only one side of each aromatic ring is involved in strong $\pi-\pi$ interactions, whereas both sides of the pyridine rings in **2** are π-stacked

Electrospray Ionization Mass Spectrometry (ESI-MS). Compound **1** contains a fairly straightforward linear Ag(I) complex that exists as an independent ion in solution. For compound **2**, the situation is less clear: can the side-on chelate with an obviously stronger nitrate interaction exist as an independent ion in solution, thus giving a "half-naked" Ag^{+} ion? High-resolution ESI-MS was used to investigate different ionic species in solution for compound **2**, and a very strong peak at m/z 228.9565 was indeed observed, consistent with the theoretical m/z calculated for the cation [Ag(pyridine-2-carboxaldoxime)]$^{+}$ (m/z 228.9526 for $C_6H_6N_2AgO$), confirming

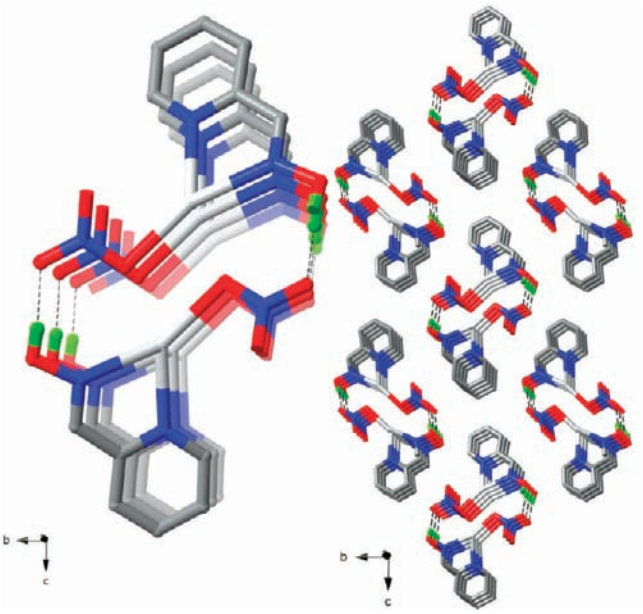

Figure 4. Left: The hydrogen-pattern (dashed lines) in **2**, giving a helical chain running in the *a* direction with additional $\pi-\pi$ interactions with interplanar distances of 3.634 Å and tilt angles of 17.9−22.5°. Right: Packing of the chains. Hydrogen atoms not participating in hydrogen bonds have been omitted. See also Table 2.

(45) McKinnon, J. J.; Spackman, M. A.; Mitchell, A. S. *Acta Crystallogr., Sect. B* **2004**, *60*, 627.
(46) Spackman, M. A.; Jayatilaka, D. *CrystEngComm* **2009**, *11*, 19.
(47) Spackman, M. A.; McKinnon, J. J. *CrystEngComm* **2002**, 378.
(48) Wolff, S. K.; Grimwood, D. J.; McKinnon, J. J.; Jayatilaka, D.; Spackman, M. A. *CrystalExplorer*, version 2.1; University of Western Australia: Perth, Australia: 2007. http://hirshfeldsurface.net/ (accessed Sep 2010).

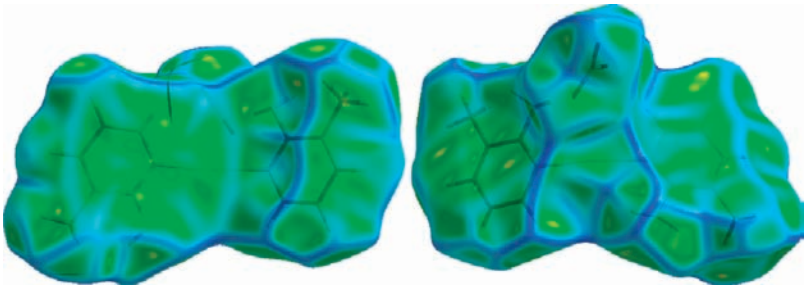

Figure 5. Hirshfeld surfaces with the curvedness mapped of one [Ag(2-amino-3-methylpyridine)$_2$]NO_3 entity in **1**, back and front view. (The nitrate group is protruding from the surface in the right plot.)

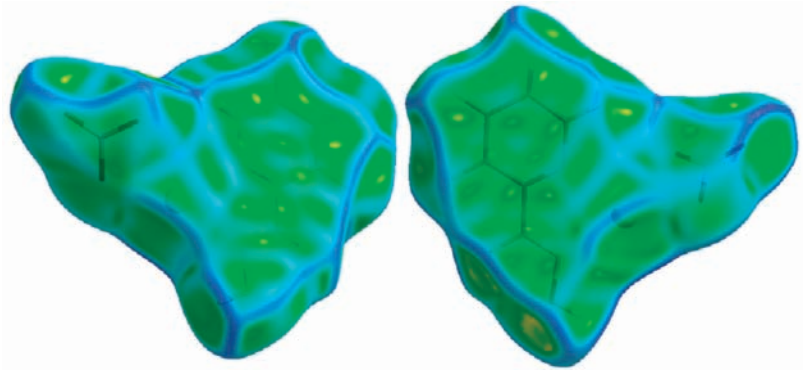

Figure 6. Hirshfeld surfaces with the curvedness mapped of one [Ag(pyridine-2-carboxaldoxime)NO_3] entity in **2**, back and front view.

Table 3. Comparison between Calculated Bond Distances and Bond Angles and the Corresponding Values from the X-Ray Structures of **1** and **2**

compound **1**			compound **2**		
bond distance	X-ray (Å)	DFT (Å)	bond distance	X-ray (Å)	DFT (Å)
Ag1−O12	3.438 (7)	2.523	Ag−O1	2.329(18)	2.278
Ag1−O13	2.828(6)	2.535	Ag−N1	2.327 (2)	2.381
Ag1−N1B	2.168 (6)	2.318	Ag−N8	2.367(2)	2.531
Ag1−N1A	2.177 (5)	2.319			
bond angle	X-ray (deg)	DFT (deg)	bond angle	X-ray (deg)	DFT (deg)
N1B−Ag1−N1A	153.2 (2)	150.2	O1−Ag−N1	129.34(7)	139.03
			O1−Ag−N8	158.88(7)	152.43
			N1−Ag−N8	71.65(7)	68.54

its presence in solution. Also, the observation of a characteristic $^{107}Ag/^{109}Ag$ isotopic peak doublet further identified this compound. However, in addition to this major peak, four solvated species with the characteristic $^{107}Ag/^{109}Ag$ isotopic peak doublet were also observed, and we assign these to the following cations: [Ag(pyridine-2-carboxaldoxime)$(H_2O)_2$]$^+$, [Ag(pyridine-2-carboxaldoxime)(DMSO)]$^+$, [Ag(pyridine-2-carboxaldoxime)(DMSO)(EtOH)]$^+$, and [Ag(pyridine-2-carboxaldoxime)(DMSO)(EtOH)]$\cdot 2H_2O^+$. The last species probably contains water hydrogen-bonded to the hydroxyl group.

DFT Calculations. As stated previously, the approximately linear (for **1**) versus chelate (for **2**) structures and the difference in nitrate interaction between the complexes in these structures questions the nature of the Ag−O bonds in these compounds. In order to determine the degree of the silver−nitrate interaction as a consequence of crystal packing and the coordinating abilities of the Ag(I) ion, DFT calculations were performed.

Pertinent bond distances and bond angles comparing experimental and calculated optimized molecular structures for the complexes in **1** and **2** are given in Table 3.

The Ag−N distances differ by 0.05−0.16 Å, and in view of some recent results of similar DFT calculations on Ag(I) complexes, this discrepancy is not surprising.[49−51] Biju and Rajasekharan found optimized bond distances for the bipyridine and phenanthroline complexes to differ within 0.14 Å of the crystallographic values, and for the corresponding 4,5-diazafluoren-9-one complex, the differences were even larger.[52] It is perhaps significant that these structures, to varying degrees, have Ag···O interactions with a nitrate anion, and that these, and the surrounding crystal packing effects, may play a significant role that is difficult to model with a simple DFT calculation. In the 4,5-diazafluoren-9-one case, there are also two different crystal

(49) Hambley, T. W.; Lindoy, L. F.; Reimers, J. R.; Turner, P.; Wei, G.; Widmer-Cooper, A. N. *J. Chem. Soc., Dalton Trans.* **2001**, 614.
(50) Liu, C. S.; Chen, P. Q.; Yang, E. C.; Tian, J. L.; Bu, X. H.; Li, Z. M.; Sun, H. W.; Lin, Z. Y. *Inorg. Chem.* **2006**, *45*, 5812.
(51) Yu, Q.; Wei, Z. Z.; Li, J. R.; Hu, T. L. *J. Mol. Struct.* **2009**, *931*, 68.
(52) Biju, A. R.; Rajasekharan, M. V. *Polyhedron* **2008**, *27*, 2065.

structures reported,[53] containing two very dissimilar [Ag(4,5-diazafluoren-9-one)$_2$]$^+$ complexes. In contrast, but perfectly consistent with this discussion, the almost perfectly linear coordination geometry with negligible nitrate interaction reported by Zhou et al. is well reproduced by their DFT calculations.[54]

These data confirm that a bent N−Ag−N geometry invites a closer Ag···O interaction, with a 10% decrease in the Ag···O distance, about the same difference as observed in a compilation of structural data.[43] The relatively large discrepancies between the calculated Ag···O "bonds" and the X-ray data are likely the effect of the "pull" of many other interactions, in particular hydrogen bonds, on the nitrate in the crystal, thus giving longer distances. We note that the geometry of the organic part of the complexes is adequately described by the methods used.

Thermal Analysis. The TG curves of **1** and **2** are shown in Figure S1 in the Supporting Information. Both compounds lose their ligands first, with an estimated mass loss of 55.60% (calculated mass loss, 56.01%) for **1** and 42.20% (calculated mass loss, 41.78%) for **2**. The final residue is probably silver metal or silver(I) oxide or a mixture thereof, giving for **1**, 20.8% (calcd, 27.9% for Ag and 30.0% for Ag_2O) and for **2**, 34.8% (calcd, 37.1% for Ag and 39.8% for Ag_2O). Although the final state is unclear, the loss of a ligand as a first step seems indisputable, and moreover, the decomposition of compound **2** clearly occurs at a higher temperature than for **1**. We tentatively attribute this to the chelate effect.

Antimicrobial Activity. Bacteria used in this investigation were of two categories: standard bacteria from the American Type Culture Collection (ATCC) and clinical bacteria, all multidrug resistant, isolated from diabetic foot ulcers by swabbing techniques. The minimum inhibition concentrations (MIC) of compounds **1** and **2** were determined and compared with 17 antibiotics used for the treatment of such foot ulcer infections, see Table 4.

[Ag(2-amino-3-methylpyridine)$_2$]NO_3 (**1**) and [Ag(pyridine-2-carboxaldoxime)NO_3] (**2**) were active against all tested bacterial strains except the standard *E. coli* (ATCC 8739) and comparable to the broad spectrum antibiotics used as references. Of the two ligands, 2-amino-3-methylpyridine is slightly active, notably against *E. coli* (ATCC 8739), while pyridine-2-carboxaldoxime is not active at all. Compounds **1** and **2** were especially efficient against *S. lutea* (MIC value 2 μg/mL for **1** compared to 4 μg/mL for the best performing amikacin and ciprofloxacin) and *M. luteus* (MIC value 4 μg/mL for **1** compared to 8 μg/mL for the best performing amikacin and cefepime) and also highly active against *S. aureus* and *K. pneumoniae*. An additional advantage of silver compounds is that they, in contrast to antibiotics in general, are active against fungi. Thus, both **1** and **2** were active against the yeast *C. albicans*. The activity of 2am3Mepy is perhaps not so surprising, as pyridine amines are generally know to be toxic, although substituted ones less so.[55] Nevertheless, it is interesting to note that the antibacterial property of this ligand against the standard *E. coli* is completely masked when bound to silver.

Because the bacterial strains are likely different, MIC values cannot be compared reliably between different bioassays. Nevertheless, without making a direct numerical comparison, we still want to mention a few recent relevant results of silver(I) complexes recently synthesized and tested. Nomiya et al. reported high activities for [Ag(imidazole)$_2$](NO_3), [Ag(1,2,4-triazole)]$_n$, and [Ag(tetrazole)]$_n$ against both *S. aureus* and *P. aeruginosa* (MIC 15.7, 7.9, and 15.7 and 7.9, 7.9, and 15.7 μg/mL, respectively) when compared to those of $AgNO_3$ (MIC 62.5 μg/mL for both bacteria).[56] [Ag(imidazole)]$_n$ and {[Ag(L-histidine)]$_2$}$_n$ were equally active against *P. aeruginosa* and *S. aureus* (MIC 12.5 and 15.7 μg/mL), while [Ag(1,2,3-triazole)]$_n$ showed no activity against these bacteria.[29] Zhang and co-workers investigated [Ag((8-pyridin-3-yl)methylthio)quinoline]$^+$ with different counterions, and higher activities were recorded for $CF_3CO_2^-$ against *S. aureus* and *P. aeruginosa* compared to NO_3^- and $CF_3SO_3^-$ (MIC 0.25 and 0.06 μg/mL), but these compounds were, just as **1** and **2**, inactive against standard *E. coli* bacteria.[57]

Our research group recently reported antimicrobial activities of Ag(I) nicotinate compounds[34] where [Ag_2-μ-O,O′-(2-aminonicotinium)$_2$-(NO_3)$_2$]$_n$ and [Ag(isonicotinamide)$_2$-μ-O,O′(NO_3)]$_2$ showed considerable activity against *P. aeruginosa* (MIC values 2−8 μg/mL), [Ag(ethyl nicotinate)$_2$](NO_3) against *S. aureus* (MIC 4−16 μg/mL), and *S. pyogenes* (MIC 2−4 μg/mL). [Ag(ethylnicotinate)$_2$](NO_3), [Ag(methylisonicotinate)$_2$(H_2O)](NO_3), and [Ag(ethylisonicotinate)$_2$-(NO_3)] showed remarkable activities against *P. mirabilis* (MIC 1−16 μg/mL).

In comparing the simple silver salt $AgNO_3$ with compounds **1** and **2**, an important parameter not immediately available from Table 4 is the activity per silver ion. Less silver in a wound dressing but with the same proficiency to kill bacteria is good because it minimizes silver waste problems and may also have a cost-reducing effect on the price of the dressing. In Table 5, we present the MIC values as micrograms of silver per milliliter for $AgNO_3$, **1**, and **2**. It can be seen that **1** and **2** have up to a factor of 10 times better silver efficiency against certain bacteria and a factor of 30 against yeast, with an average improvement against all microorganisms of 3.9. The most efficient compound seems to be **1**, outperformed by $AgNO_3$ only on two of 18 tested strains.

Electrophoretic DNA Migration. The antibacterial action of silver ions on the molecular level is not known in detail, but three basic mechanisms have been proposed: (1) interference with electron transport, (2) interaction with the cell membrane, and (3) binding to DNA.[58] That silver(I) ions in the form of silver nitrate do indeed interact with DNA was shown more than 40 years ago;[59,60] however, silver(I) complex ions may have different effects, as shown for the silver

(53) Massoud, A. A.; Gohar, Y.; Langer, V.; Lincoln, P.; Svensson, F. R.; Jänis, J.; Gårdebjer, S. T.; Haukka, M.; Jonsson, F.; Aneheim, E.; Löwenhielm, P.; Abu-Youssef, M. A. M.; Öhrström, L. To be submitted **2010**.
(54) Zhou, C. H.; Zhu, H. Y.; Wang, Y. Y.; Liu, P.; Zhou, L. J.; Li, D. S.; Shi, Q. Z. *J. Mol. Struct.* **2005**, *779*, 61.
(55) Scriven, E. F. V.; Murugan, R. Pyridine and Pyridine Derivatives. In *Kirk-Othmer Encyclopedia of Chemical Technology*; John Wiley & Sons, Inc.: Hoboken, NJ, 2005.
(56) Kasuga, N. C.; Yamamoto, R.; Hara, A.; Amano, A.; Nomiya, K. *Inorg. Chim. Acta* **2006**, *359*, 4412.
(57) Zhang, J.-A.; Pan, M.; Zhang, J.-Y.; Zhang, H.-K.; Fan, Z.-J.; Kang, B.-S.; Su, C.-Y. *Polyhedron* **2009**, *28*, 145.
(58) Lopez-Garzon, R.; Romero-Molina, M. A.; Navarrete-Guijosa, A.; Lopez-Gonzalez, J. M.; Alvarez-Cienfuegos, G.; Herrador-Pino, M. M. *J. Inorg. Biochem.* **1990**, *38*, 139.
(59) Yamane, T.; Davidson, N. *Biochim. Biophys. Acta* **1962**, *55*, 609.
(60) Nordén, B.; Matsuoka, Y.; Kurucsev, T. *Biopolymers* **1986**, *25*, 1531.

Table 4. Minimum Inhibitory Concentration (MIC) for **1**, **2**, Ligands, and $AgNO_3$, against Multidrug Resistant Bacteria Isolated from Diabetic Foot Ulcers Compared with Those of a Number of Commercial Antibiotics[a]

	Gram-positive bacteria						Gram-negative bacteria											
antibiotic	*S. luted*[b]	*M. luteus*[c]	*S. aureus*[d]	*S. aureus* 1[c]	*S. aureus* 2[c]	*S. pyogenes*[c]	*E. coli*[e]	*E. coli*[c]	*K. pneumoniae*[c]	*P. aeruginosa*[f]	*P. aeruginosa* 1[c]	*P. aeruginosa* 2[c]	*P. aeruginosa* 3[c]	*P. mirabilis* I[c]	*P. mirablis* II[c]	*E. cloacae*[c]	*S. enterica*[c]	*C. albicans*[c]
	MIC (μg/mL)																	
amikacin	4	8	4	32	64	256	8	32	256	4	12	32	256	128	64	256	256	
gentamicin	16	16	16	16	32	64	4	*16*	32	12	24	24	96	32	192	256	64	
streptomycin	16	64	12	64	128	128	6	32	64	8	16	12	128	64	128	256	32	
amoxicillin	8	24	8	16	32	96	32	192	256	8	256	16	192	256	192	128	256	
ampicillin	64	16	4	*8*	16	64	24	64	256	4	*8*	*8*	96	256	128	96	256	
cephradine[i]	48	64	16	12	64	128	24	128	192	16	128	32	192	96	192	256	*8*	
cefuroxime[ii]	32	32	8	24	32	256	16	64	128	8	64	16	128	64	96	128	12	
cefoperazone[iii]	16	16	6	16	32	128	12	24	96	32	*8*	16	96	32	32	48	24	
cefepime[iv]	24	8	4	*8*	12	32	4	32	64	8	32	*8*	48	*24*	*24*	32	12	
imipenem	8	32	*2*	16	16	196	3	*16*	256	8	256	64	96	256	256	16	32	
Meropenem	32	16	*2*	12	*8*	128	*2*	64	192	4	128	48	64	128	128	*12*	16	
azithromycin	16	16	12	24	16	64	12	32	64	12	128	64	128	96	48	64	96	
clarithromycin	24	24	16	32	*8*	48	8	24	32	8	96	48	96	64	32	32	48	
nalidixic acid [i]	8	32	24	64	64	128	4	*16*	128	8	64	48	128	192	256	256	32	
ciprofloxacin[ii]	4	24	4	48	32	64	6	32	32	4	48	24	64	128	64	128	32	
levofloxacin[iii]	16	16	3	32	16	*16*	8	24	16	*2*	32	16	*32*	48	32	32	128	
vancomycin	32	24	32	16	32	64	4	32	128	32	64	32	128	128	48	64	256	
$AgNO_3$	8	12	24	12	24	*16*	24	32	16	64	48	24	96	64	48	16	12	48
2am3Mepy	32	24	48	24	128	48	24	64	96	256	128	96	64	256	128	64	48	256
1	*2*	4	16	*8*	64	*16*	256	64	*8*	64	32	16	64	32	64	16	*8*	*8*
py2ald	256	256	256	256	256	256	256	256	256	256	256	256	256	256	256	256	256	256
2	16	*2*	4	16	16	32	256	64	16	128	32	16	*32*	32	32	32	16	*4*

[a] Italic font indicates the best performing substance(s) for each strain (MIC ≥ 256). [b] ATCC 10031. [c] Clinical. [d] ATCC 6538p. [e] ATCC 8739. [f] ATCC 9027 Roman superscript numbers (i−iv) indicate the generation of the antibiotic.

Table 5. Average Minimum Inhibitory Concentration (MIC) from Table 4 for $AgNO_3$, **1**, and **2** Expressed as Micrograms of Silver per Milliliter[a]

	Gram-positive bacteria						Gram-negative bacteria								
antibiotic	*S. lutea*[b]	*M. luteus*[c]	*S. aureus*[d]	*S. aureus* 1[c]	*S. aureus* 2[c]	*S. pyogenes*[c]	*E. coli*[c]	*E. coli*[c]	*K. pneumoniae*[c]	*P. aeruginosa*[f]	*P. aeruginosa* 1[c]	*P. aeruginosa* 2[c]	*P. aeruginosa* 3[c]	*P. mirabilis* I[c]	*P. mirabilis* II[c]	*E. cloacae*[c]	*S. enterica*[c]	*C. albicans*[c]
MIC (μg(Ag)/mL)																		
$AgNO_3$	5.1	7.6	15.2	7.6	15.2	10.2	15.2	20.3	10.2	40.6	30.5	15.2	61.0	40.6	30.5	10.2	7.6	30.5
1	*0.6*	*1.1*	*4.5*	*2.2*	*17.9*	*4.5*	*71.5*	*17.9*	*2.2*	*17.9*	*8.9*	*4.5*	*17.9*	*8.9*	*17.9*	*4.5*	*2.2*	*2.3*
2	*5.9*	*0.7*	*1.5*	*5.9*	*5.9*	*11.8*	*94.6*	*23.6*	*5.9*	*47.3*	*11.8*	*5.9*	*11.8*	*11.8*	*11.8*	*11.8*	*5.9*	*1.5*

[a] Italic font indicates cases where **1** or **2** outperforms $AgNO_3$.

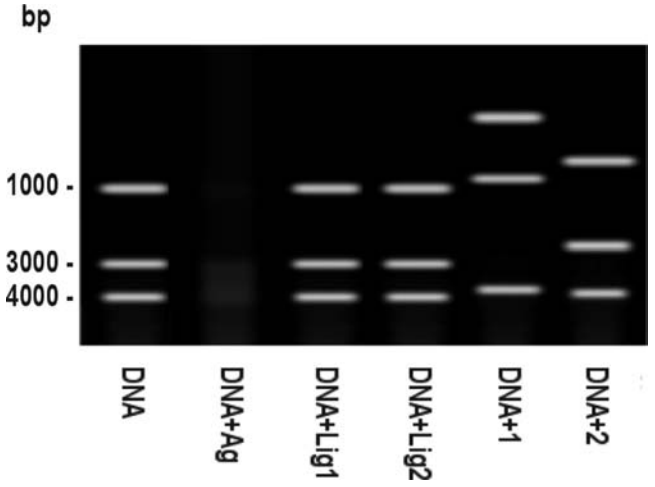

Figure 7. Electrophoretic DNA (1 μg) migration in the absence (lane 1) and presence of 2 μg of silver nitrate (Ag), 2am3Mepy (Lig 1), py2ald (Lig2), **1**, and **2**. (DNA chains were stained with ethidium bromide.)

sulfadiazine compound.[61] The lack of solution chemistry data in physiologically relevant media is troublesome, as it is not firmly established whether the active species in antibacterial studies of silver(I) compounds are indeed Ag(I) complexes, if the effect is somehow only mediated by the ligands, or if it is simply a question of the solubility of the compounds. On one hand, potentiometrically determined stability constants for 1:1 and 1:2 complexes of Ag^+ and pyridine in 0.1 mol·dm^3 tetraethylammonium perchlorate DMSO solutions[62,63] are rather small, i.e., $\log K_1 = 1.41$,[63] so that our solutions may in fact contain various amounts of uncomplexed silver ions, and in higher proportion as the dilution increases.[64] On the other hand, silver sulfadiazine has been shown to act as an "undissociable molecule" in complexation studies with DNA.[61] Moreover, it is not evident how to extrapolate the 0.1 M ionic strength data to 100% DMSO, or indeed to physiological relevant water solutions, so further studies of the aqueous chemistry are needed.

Shifts in solution NMR are good indicators of complex formation, and we have also established that the complex ion of **2** and corresponding solvated species are stable under ESI-MS conditions. The biological activity is not simply a question of solubility of the compounds, as **1** is 8 times more active than **2** against *S. lutea*, whereas **2** is 4 times more active than **1** against two of the *S. aureus* strains.

In order to further investigate the solution chemistry, and the possible DNA interaction, we performed DNA coupling experiments where 1 μg of DNA was incubated with 2 μg of 2am3Mepy, py2ald, silver nitrate, **1**, or **2** and then migrated in an electrophoresis experiment. The results, shown in Figure 7, indicate a different effect of the two compounds, different from that of the ligands or silver nitrate. Thus, mimicking a biologically relevant solution, the two complexes show different interactions with a biological molecule that is a possible target for the antibacterial effect.

(61) Rosenkranz, H. S.; Rosenkranz, S. *Antimicrob. Agents Chemother.* **1972**, *22*, 373.
(62) Grzejdziak, A.; Olejniczak, B.; Seliger, P. *J. Mol. Liq.* **2002**, *100*, 81.
(63) Cassol, A.; Dibernardo, P.; Zanonato, P.; Portanova, R.; Tolazzi, M. *J. Chem. Soc., Dalton Trans.* **1987**, 657.
(64) Dorn, T.; Fromm, K. M.; Janiak, C. *Aus. J. Chem.* **2006**, *59*, 22.

Moreover, the staining of the DNA chains was made with ethidium bromide, and with $AgNO_3$ (lane 2 in Figure 7), clearly some unwanted side reaction takes place, such as the precipitation of the very insoluble AgBr(s). On the contrary, the distinct pattern in lanes 5 and 6 indicates the integrity of the complex ions in **1** and **2**.

Conclusions

[Ag(2-amino-3-methylpyridine)$_2$]NO_3 (**1**) and [Ag(pyridine-2-carboxaldoxime)NO_3] (**2**) have fundamentally different structures, a linear complex ion in **1** and a "half-naked" chelate in **2**, the existence of the latter confirmed by ESI-MS. DFT-ZORA calculations reproduce the geometry and vibrational frequencies of both **1** and **2** fairly well. The two compounds show antibacterial effects against different bacteria and yeast, quite comparable to commercial antibiotics *in vitro*, but their activity spectrum is different, on both a microgram per milliliter basis and a Ag per milliliter basis. We cannot with certainty attribute this to the different complex ions in solution, but this idea is corroborated by electrophoretic DNA migration showing different interaction patterns for **1** and **2** compared to those of the free ligands or silver nitrate.

Acknowledgment. This work was supported by the Swedish International Development Agency (SIDA) through the Swedish Research Links Program and Kungliga Vetenskaps och Vitterhetssamhället i Göteborg. We are thankful to Prof. Janne Jänis, University of Eastern Finland, for help with the ESI-MS measurements, to Dr. Raja Dey for assistance with the X-ray data collection, and to Ms. Alshima'a A. Massoud for help with the preparations.

Supporting Information Available: Crystallographic information files (CIF) for **1** and **2** and a plot of TGA data. This material is available free of charge via the Internet at http://pubs.acs.org.